Effect of dispersed silica particles on the smectic-*A*−smectic-*C** phase transition

Z. Kutnjak,[1] S. Kralj,[2,1] and S. Žumer[3,1]

[1]*Condensed Matter Physics Department, Jožef Stefan Institute, Jamova 39, 1000 Ljubljana, Slovenia*
[2]*Laboratory of Physics of Complex Systems, Faculty of Education, University of Maribor, Koroška 160, 2000 Maribor, Slovenia*
[3]*Department of Physics, Faculty of Mathematics and Physics, University of Ljubljana, Jadranska 19, 1000 Ljubljana, Slovenia*
(Received 27 May 2002; published 9 October 2002)

We study the influence of the dispersed aerosil particle concentration on the soft and Goldstone mode dynamics across the smectic-*A*−smectic-*C** phase transition using dielectric spectroscopy. We use CE8 liquid crystal filled with aerosils of concentrations $x = m_s/(m_s + m_{LC}) = 0.025$, 0.05, 0.1, and 0.15, where m_s and m_{LC} stand for masses of aerosil and liquid crystal, respectively. In dispersions with $x < 0.15$ the characteristic Goldstone frequency temperature dependence $f_G(T)$ is almost bulklike in contrast to the corresponding soft mode dependence $f_s(T)$. For $x > 0$ the degeneracy of the modes at the Sm*A*-Sm*C** transition temperature is lifted. With increasing x the modes' intensities gradually decrease and the critical effective coefficient γ tentatively approaches the value characterizing the three-dimensional *XY* universality class. For $x = 0.15$, a drastic change in behavior is observed. The Goldstone mode is completely suppressed and the $f_s(T)$ dependence begins to deviate from the Arrhenius behavior. A simple phenomenological approach is used in the explanation of results.

I. INTRODUCTION

Phase behavior influenced by irregular confinement has been an interesting topic for years. Convenient experimental systems to study this phenomenon are numerous liquid crystal (LC) phases either confined to various porous matrices [1] or filled with inclusions [2]. The choice of various LC phases is justified by a rich variety of different phase transitions that they exhibit in translational or orientational long range ordering [3]. In addition LCs are typical representatives of soft systems characterized by a strong response to relatively weak perturbations. Among the confining matrices acting as disordering agents, controlled-pore glasses (CPG), Vycor glasses, millipore membranes, or aerogels are conventionally used [1]. In these matrices the degree of randomness (i.e., geometrically enforced disorder) gradually increases from the former (CPG) to the latter (aerogel) system. As inclusions, aerosil particles (spherular SiO$_2$ objects) of diameter 2 R $\sim$ 7 nm, whose surface is covered by hydroxyl groups, are typically used [2].

By varying the aerosil particles concentration ρ_s (weight of silica per cm^3 of LC), the degree of disordering enforced to a hosting LC phase can be relatively well controlled. On increasing ρ_s the organization of aerosil particles undergoes three qualitatively different regimes [2,4,5]. Below the gelation threshold $\rho_s = \rho_g \sim 0.01$ g/cm^3, almost isolated aggregates of aerosil float in LCs. Above ρ_g the gel-like aerosil structure is formed that is enabled by hydrogen bonding between hydroxyl groups on aerosil surfaces. For densities ρ_s less than $\rho_a \sim 0.1$ g/cm^3 this structure is relatively responsive. If the elastic strain imposed by surrounding LC phase is large enough the bonds among aerosil particles relatively, break easily and rearrange allowing partial relaxation of the strain. The regime $\rho_s < \rho_a$, in which the induced disorder can be partially annealed, is referred to as the *soft* or also the *annealed strain* regime. For larger concentrations the *stiff* regime is entered resembling the rigid aerogel structure.

There the geometrically induced disorder is almost fully quenched.

In studying the influence of ρ_s on LC phase behavior most studies so far focused on the isotropic-nematic (*I-N*) and nematic-smectic *A* (*N*-Sm*A*) phase transitions [2,5–10].

In general the observed phase transition temperature shifts towards lower temperatures [2] are relatively large and exhibit nonmonotonous ρ_s dependence, reflecting qualitative changes in the aerosil arrangement. In the regime $\rho_s < \rho_a$ in the nematic phase bimodal behavior is often observed [5]. The first contribution resembles the bulk behavior. On the contrary the second one is more or less glasslike, originating from LC molecules in strong contact with the aerosil network. Thermal anisotropy studies [9] indicate that the aerosil inclusions break the system into strongly polydomain orientational ordering. With increasing ρ_s the character of the *N*-Sm*A* transition as a rule approaches three-dimensional *XY* universality class [2]. This indicates that the increased disorder weakens the coupling between the nematic and smectic order parameters. For $\rho_s > \rho_a$ a strong change in the qualitative behavior is observed resembling the behavior of LCs confined to aerogels matrices. In this regime the *I-N* and *N*-Sm*A* specific heat peaks become anomalously broadened [2]. For even larger concentrations ($\rho_s \gtrsim 0.4$ g/cm^3) the disorder is expected to completely smear out the discontinuous *I-N* phase transition [2,11].

In this contribution we study the influence of aerosil concentration on the Sm*A*-Sm*C** phase transition. This phase transition has been intensively studied in bulk. In addition to studies of critical phenomena [13,12], which are driven by an interest in basic physics, electro-optic applications have also been explored [14]. In most cases the bulk Sm*A*-Sm*C** phase transition is expected to be of second order what is predicted by molecular theories [15] (Note that the interaction between different order parameter fluctuation may change the second-order character of the transition [16].) Its main characteristics can be described with the two component order parameter [17,18], often defined with angles θ and

ϕ. Here θ describes deviations of molecular orientation from the smectic layer normal and the ϕ defines the molecular projection in the layer plane. The dynamics of the second-order smectic-A–smectic-C^* phase transition taking place at $T = T_{AC}$ is dominated by the doubly degenerated soft mode at $T \geq T_{AC}$. Below the transition this degeneracy is lifted, bifurcating into the Goldstone mode and soft amplitude mode [17]. The first, the symmetry recovering mode, is below T_{AC} dominant and describes fluctuations in ϕ. The amplitude mode describes fluctuations in θ.

In this contribution we focus on the influence of aerosil concentration on the dynamics of the soft and Goldstone mode of the SmA-SmC^* phase transition in the CE8 (8CI*) liquid crystal by means of the dielectric spectroscopy. The plan of the paper is as follows. In Sec. II we present the experimental setup. In Sec. III the model used to explain the measurements presented in Sec. IV is briefly given. The results are discussed in Sec. V and summarized in the last section.

II. EXPERIMENTAL SET UP

We studied a mixture S-($+$)- [4-(2$'$-methylbutyl) phenyl 4$'$-n-octylbiphenyl-4-carboxylate] (denoted as CE8 or 8SI*) ferroelectric LC and Degussa hydrophilic aerosil A 300 [19,2]. The aerosil consists of nearly spherical SiO$_2$ particles of diameter 2 R$\sim$7 nm with fairly narrow size distribution (full width at half maximum of distribution $\sim$7.5 nm). They are covered with -OH (hydroxyl) groups that can bond hydrogen in a network at a high enough concentration. The hydrophilic coating produces [4] a strong homeotropic anchoring (i.e., tends to orient molecules along the surface normal) of polar LC molecules at the surface. The quoted specific surface area is 300 m^2/g. The CE8-aerosil mixtures were prepared with the solvent method [7] by using chemically pure acetone. After slow evaporation of the acetone the mixture was placed in vacuum for one hour to remove the remaining acetone. During this procedure the sample was kept in the SmA phase, i.e., it was not allowed to enter the crystal phase.

Four different mixtures were prepared with $x = 0.025, 0.05, 0.10,$ and 0.15. Here $x = m_s / (m_s + m_{LC})$, where m_s and m_{LC} are masses of aerosils and liquid crystal in the mixture, respectively. Note that we use relative mass concentration x instead of density $\rho_s = (m_s/m_{LC})\rho_{LC}$ of silica in liquid crystal quoted in other studies because x is not temperature dependent. Here $\rho_{LC} \sim 1$ g/cm^3 is the density of the liquid crystal material.

The complex dielectric constant $\varepsilon^*(T,\omega) = \varepsilon' - i\varepsilon''$ was measured using HP4282A LCR meter. The method is described in Ref. [20]. The LC is confined within a plane parallel cell of thickness $d \sim 50$ μm. For latter convenience we introduce the Cartesian coordinate system, where cell plates are set at $y = 0$ and $y = d$. In bulk, the layers are stacked along the z direction in the so-called bookshelf arrangement. This was achieved by orienting the sample in the magnetic field of strength 9 T on cooling the sample through the I-N transition. The electric field is applied along the cell plates

normal in the y direction. The amplitude of the excitation voltage was 1 V.

In scanning runs, the dielectric constant was measured at few frequencies between 40 Hz and 4 kHz on cooling the sample with the typical cooling rate of 200 mK/h. In the temperature stepping run the dielectric spectra were taken at 60 frequencies between 20 Hz and 1 MHz on cooling the sample with typical temperature steps of -50 mK.

III. THEORETICAL BACKGROUND

Let us first consider the bulk system with layers in the bookshelf geometry. The orientational ordering of a molecule is given by the nematic director field

$$\vec{n} = (\sin \theta \cos \phi, \sin \theta \sin \phi, \cos \theta). \quad (1)$$

In the SmA phase $\theta = 0$. In the equilibrium SmC^* phase the molecules are tilted from smectic layers for the cone angle $\theta = \theta_0$ and the molecules precess around the cone as $\phi = \phi_0 = q_0 z$. Here $p = 2\pi/q_0$ represents the pitch of the helix. The values of θ_0 and q_0 result from the minimization of the relevant free energy [18,21].

Note that as a primary orientational order parameter of the SmA-SmC^* phase transition one conventionally introduces a two component parameter [17,18] $\vec{\xi} = (\xi_1, \xi_2)$:

$$\xi_1 = n_x n_z \sim \theta \cos \phi, \quad \xi_2 = n_y n_z \sim \theta \sin \phi. \quad (2)$$

In this approach one assumes that layers adopt the equilibrium spacing. In the SmC^* phase the tilt locally breaks the axial symmetry and introduces a transverse in-plane spontaneous polarization $\vec{P} = (P_x, P_y, 0)$ perpendicular to the direction of tilt. Therefore it holds $P_x = \text{const } n_y n_z$ and $P_y = -\text{const } n_x n_z$. In the equilibrium the average polarization of the sample is thus zero. Note that $\vec{P}$ is only a secondary order parameter which relaxes much faster than liquid crystalline degrees of freedom so that one can use adiabatic approximation and renormalize material constants [22]. This is justified for calculations of the equilibrium LC structures and dominant director dynamics.

With this in mind the most essential properties of the system of our interest can be obtained from the free energy density [13,18]

$$f = \frac{a_0(T - T_{AC})}{2}(\xi_1^2 + \xi_1^2) + \frac{b}{4}(\xi_1^2 + \xi_1^2)^2 - \Lambda\left(\xi_1 \frac{\partial \xi_2}{\partial z}\right.$$

$$\left. - \xi_2 \frac{\partial \xi_1}{\partial z}\right) + \frac{K_3}{2}\left(\left(\frac{\partial \xi_1}{\partial z}\right)^2 + \left(\frac{\partial \xi_2}{\partial z}\right)^2\right)^2 + \frac{K'}{2}\left(\frac{\partial \xi_1}{\partial x} + \frac{\partial \xi_2}{\partial y}\right)^2$$

$$+ \frac{K''}{2}\left(\frac{\partial \xi_1}{\partial y} - \frac{\partial \xi_2}{\partial x}\right). \quad (3)$$

Here a_0, b, Λ are the phenomenological constants and K_3, K', K'' orientational elastic constants analogous to the bend, splay, and twist, nematic Frank elastic constants, respectively. The equilibrium wave vector of the helical pitch is

given by $q_0 = \Lambda / K_3$. To obtain the dynamics of the order parameter fluctuations one introduces the dissipation function density as [13]

$$f_d = \frac{\nu}{2} \left(\left(\frac{\partial \xi_1}{\partial t} \right)^2 + \left(\frac{\partial \xi_2}{\partial t} \right)^2 \right). \tag{4}$$

The characteristic viscous coefficient ν is expected to exhibit noncritical behavior and is thermally activated [23].

Expansion of the order parameter $\vec{\xi}(\vec{r},t) \sim \vec{\xi}_{eq}(\vec{r}) + \delta \vec{\xi}(t)$ about the equilibrium profile $\vec{\xi}_{eq}(\vec{r})$ and considering Eqs. (3),(4) one obtains in the SmA phase, double degenerated soft mode. In the SmC^* phase the degeneracy is lifted and one obtains the soft amplitude mode (fluctuations in θ) and the Goldstone mode (fluctuations in ϕ). The dispersion relations [13] for the characteristic mode relaxation times as a function of the mode wave vector $\vec{q} = (q_x, q_y, q_z)$ read as

$$\frac{1}{\tau_s} = \frac{1}{\nu} [a_0 (T - T_{AC}) + K_3 (q_0 \pm q_z)^2 + K_+ q_\perp^2]; \quad T \geq T_{AC}, \tag{5a}$$

$$\frac{1}{\tau_s} = \frac{1}{\nu} [2a_0 (T_{AC} - T) + K_3 (q_0 \pm q_z)^2 + K_+ q_\perp^2]; \quad T \leq T_{AC}, \tag{5b}$$

$$\frac{1}{\tau_G} = \frac{1}{\nu} [K_3 (q_0 \pm q_z)^2 + K_+ q_\perp^2]; \quad T \leq T_{AC}. \tag{5c}$$

Here $K_+ = (K' + K'')/2$, $q_\perp^2 = q_x^2 + q_y^2$ and subscript s and G refer to the soft and Goldstone mode, respectively.

In our experiment we probe Goldstone and soft mode fluctuations with dielectric spectroscopy. This method [22,20] measures the complex dielectric constant $\varepsilon(\omega)^* = \varepsilon(\omega)' - i\varepsilon(\omega)''$ response of the polarization of the system at zero wave vector to an external homogeneous field $\vec{E} = (0,E,0)e^{i\omega t}$. In our case the dielectric response within the frequency regime studied can be approximately expressed [22] as

$$\varepsilon(\omega, T \geq T_{AC})^* = \frac{\Delta \varepsilon_s}{1 + i \omega \tau_s} + \varepsilon_\infty, \tag{6a}$$

$$\varepsilon(\omega, T \leq T_{AC})^* = \frac{\Delta \varepsilon_s}{1 + i \omega \tau_s} + \frac{\Delta \varepsilon_G}{1 + i \omega \tau_G} + \varepsilon_\infty. \tag{6b}$$

Here $\Delta \varepsilon_s$ and $\Delta \varepsilon_G$ describe the strength of the soft mode and Goldstone mode contributions, respectively, and ε_∞ includes all higher ω mode contributions. In this approximation each mode is characterized by a single relaxation time. One commonly defines the corresponding relaxation frequencies of both the modes as $f_s = 1/2\pi\tau_s$ and $f_G = 1/2\pi\tau_G$.

Below T_{AC} the dielectric response is dominated by the Goldstone mode. For the geometry described, its amplitude at $q=0$ is to a good approximation expressed as [13]

$$\Delta \varepsilon_G = \left(\frac{P}{\theta} \right)^2 \frac{\varepsilon_0}{2 K_3 q_0^2}. \tag{7}$$

IV. EXPERIMENTAL RESULTS

We have measured the complex dielectric constant $\varepsilon(\omega)^* = \varepsilon(\omega)' - i\varepsilon(\omega)''$ across the SmA-SmC^* phase transition in the aerosil filled CE8 phase. We studied mixtures with $x = 0.025, 0.05, 0.10, 0.15$ and also a reference pure bulk CE8 sample. The data were analyzed using the modified Cole-Davison ansatz,

$$\varepsilon(\omega, T \geq T_{AC})^* = \frac{\Delta \varepsilon_s}{(1 + i \omega \tau_s)^h} + \varepsilon_\infty + \frac{\sigma_R}{\omega} + \frac{i \sigma_i}{\omega}, \tag{8a}$$

$$\varepsilon(\omega, T \leq T_{AC})^* = \frac{\Delta \varepsilon_s}{(1 + i \omega \tau_s)^h} + \frac{\Delta \varepsilon_G}{(1 + i \omega \tau_G)^k} + \varepsilon_\infty + \frac{\sigma_R}{\omega}$$
$$+ \frac{i \sigma_i}{\omega}, \tag{8b}$$

where $\Delta \varepsilon_s$, $\Delta \varepsilon_G$, ε_∞, $f_s = 1/(2\pi\tau_s)$, $f_G = 1/(2\pi\tau_G)$, h, k, and the complex conductivity $\sigma^* = \sigma_R + i\sigma_i$ are the fitting parameters. Departures of powers h and k from 1 indicate distribution of the soft mode and Goldstone mode relaxation times about characteristic values τ_s and τ_G, respectively. The conductivity terms take into account finite conductivity of the system.

In Fig. 1 we show the temperature evolution of the dielectric dispersion in Cole-Cole plots for pure CE8 and different aerosil mixtures. Above T_{AC}, only soft mode is observed and below it also the Goldstone mode appears. The corresponding temperature and concentration dependent strengths of modes are plotted in Fig. 2. Both modes are increasingly suppressed with growing x. For $x = 0.15$ the Goldstone mode disappears within the experimental accuracy and the soft mode distribution broadens. Note that temperature shifts $\Delta T_{AC} = T_{AC}^{(0)} - T_{AC}(x) < 0.2$ K from the pure bulk SmA-SmC^* phase transition temperature, $T_{AC}^{(0)} = 357.90$ K are relatively small in the whole examined range [see Table I for $T_{AC}(x)$]. The characteristic frequencies as functions of T and x are plotted in Fig. 3. The two frequencies are degenerate at $T_{AC}^{(0)}$ in pure CE8. For $x > 0$ this degeneracy is lifted. Note that f_G is, relatively, weakly affected by x in comparison to f_s [24]. In Fig. 4 we plot the temperature dependent static dielectric constant for different concentrations x. The critical exponent γ revealing the character of the AC transition can be inferred. For $x = 0.15$ the $\varepsilon'(T)$ dependence exhibits a dramatic change in the behavior. For temperatures $T > T_{AC}(x)$ we fitted ε' to the scaling ansatz [25]

$$\varepsilon' = \frac{A^+}{r^\gamma} (1 + D_1^+ r^{\Delta_1}) + Br + C, \tag{9}$$

where $r = (T - T_{AC})/T_{AC}$ is the reduced temperature, A^+, D_1^+, Δ_1, B, and C are the fitting parameters. The correction
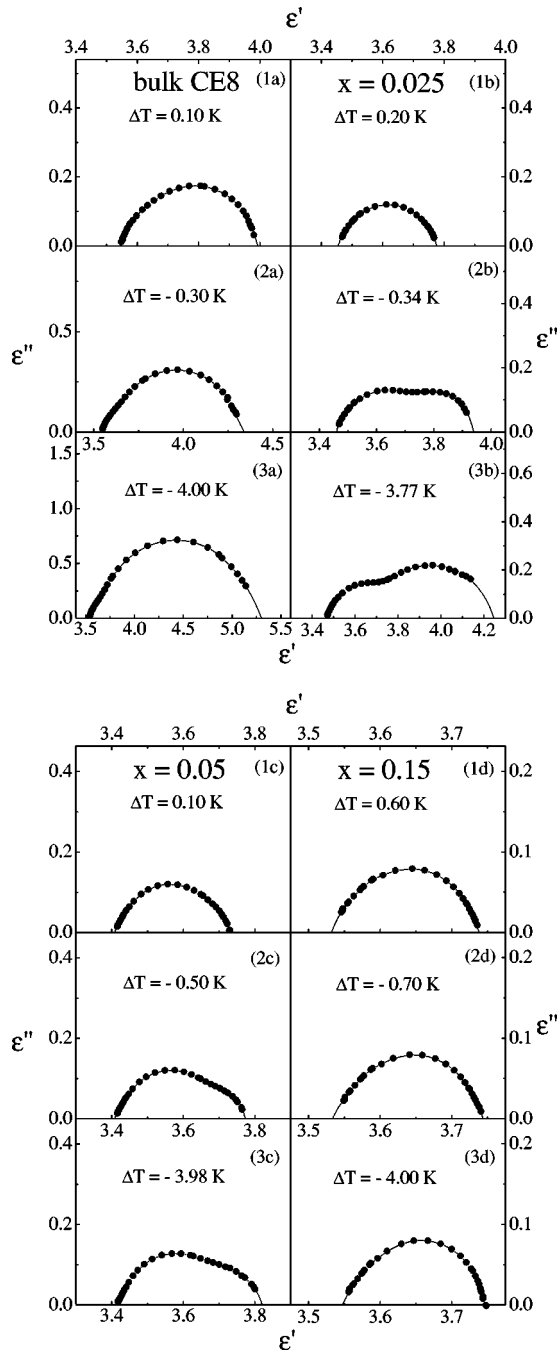
FIG. 1. Measured values of ε'' plotted versus ε' for different concentrations x and three different temperatures $\Delta T = T - T_{AC}$. (a) pure bulk sample, (b) $x = 0.025$, (c) $x = 0.05$, (d) $x = 0.15$.

to scaling factor D_1^+ was found negligibly small and set to zero and $\Delta_1 = 0.5$. Below $T_{AC}(x)$ we were not able to fit $\varepsilon'(T)$ dependence of the soft mode because in this temperature regime the dielectric response is dominated by the Goldstone mode. The results reveal (Fig. 5) that the extracted value of γ strongly depends on the temperature range used in the fitting procedure.

Note that the data in Fig. 4 were taken at 4 kHz because at this particular frequency the anomaly related to the soft mode is best visible on the slope of the increasing Goldstone
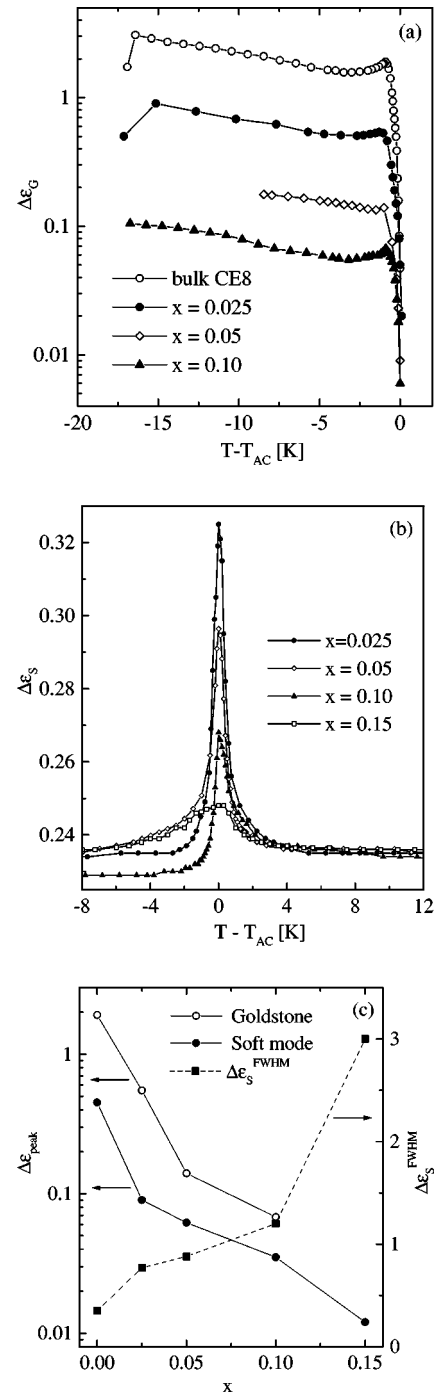

FIG. 2. Temperature dependence of the dielectric intensity $\Delta\varepsilon_{\mathrm{mod}\,e}$ of the (a) Goldstone and (b) soft mode in various LC and aerosil mixtures. The intensities of both modes are strongly suppressed with increasing x. For $x = 0.15$ the Goldstone mode disappears and the soft mode exhibits strong widening and rounding. (c) Decreasing of the peak dielectric constant with increasing x for both soft and Goldstone mode and widening of the soft mode peak.

mode dielectric intensity just below $T_{AC}(x)$ (see the narrow small peak in the first panel of Fig. 4). Data at 4 kHz are thus serving purely as an illustration. Actually it should be noted that the 4 kHz data due to the critical slowing down do not represent any more below some temperature near $T_{AC}(x)$,

TABLE I. Concentration of the aerosil particles and consequent phase transition temperature shifts, typical length scale l_0 enforced to LC and relative fraction p of frozen LC molecules for a homogeneous distribution of aerosils.

x	$T_{AC}(x)$ (K)	ρ_s (g/cm^3)	l_0 (μm)	p
0.025	357.85	0.026	0.26	0.02
0.05	357.78	0.053	0.13	0.03
0.10	357.75	0.111	0.06	0.07
0.15	357.70	0.176	0.04	0.11

the static dielectric response, which should be solely fitted to the power ansatz. This breakdown of the static response itself would introduce the additional rounding effect. So the 4 kHz data near $T_{AC}(x)$ were actually replaced progressively by the low frequency data in order to ensure the static response validity. To illustrate this problem the 1 kHz data are added to the second panel in Fig. 4 showing ε' of the $x=0.05$ mixture. Here, the small kink in the slope of 1 kHz data corresponds to the $T_{AC}(x)$ soft mode anomaly.

V. DISCUSSION

In Table I we summarize some of geometric characteristics [2] of our samples, characterized by the main aerosil void size $l_0 \sim 2/(a\rho_s)$, equivalent to the mean LC length scale and the relative fraction $p \sim a_0 a \rho_s$ of "frozen" LC molecules (i.e., molecules in strong contact with the aerosil particles). To estimate values of l_0 and p we set $a \sim 300$ g/cm^3 and $a_0 \sim 2$ nm. These estimates assume homogeneous distribution of aerosil particles.

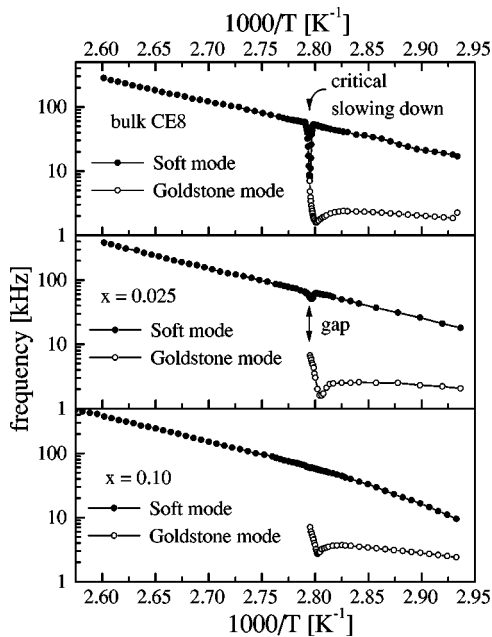For all concentrations studied the estimated value of l_0 is

FIG. 3. Temperature dependence of the characteristic relaxation frequencies. Note the degeneracy of the two frequencies at T_{AC} in pure CE8 and appearance of the gap at $x>0$.
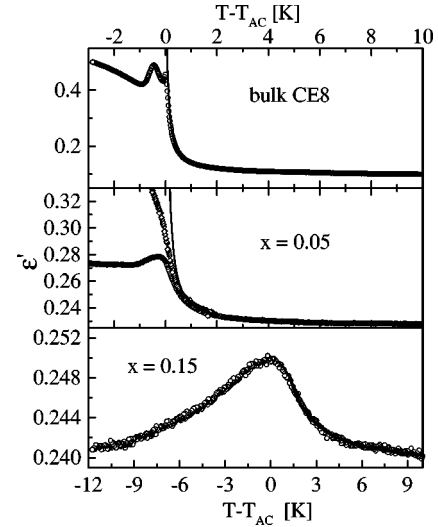

FIG. 4. The temperature variation of the dielectric constant at 4 kHz (open circles) and for $x=0.05$ also at 1 kHz (diamonds). Solid lines represent fits of the static dielectric constant to the scaling ansatz.

well below the pitch of the helix (~ 2 μm). The aerosil particles are known to strongly anchor the LC molecules [4]. Therefore they are expected to strongly pin the fluctuations and thus suppress fluctuations with wave vector $q \neq N\pi/l_0$, where $N=1,2,3,\ldots$. Note that our measurements were performed at $q \sim 0$ and consequently one would expect complete suppression of measured modes for all concentrations of aerosils studied. This should particularly affect the Goldstone modes because ϕ is said to be the "soft" component of the order parameter: i.e., its spatial variation readily adopts to the imposed geometrical length scale.

However results for $x<0.15$ disagree with these expectations. The Goldstone mode amplitude (Fig. 2) remains finite
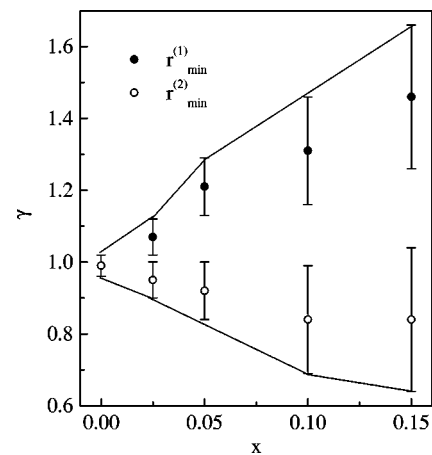

FIG. 5. Effective critical exponent γ for two limiting temperature ranges. Solid lines represent also the range of critical exponents within 95% confidence level. $r_{min}^{(1)}(x=0-0.05) \sim 2\times10^{-3}$, $r_{min}^{(2)}(x=0-0.05) \sim 5\times10^{-4}$, $r_{min}^{(1)}(0.10) \sim 2.7\times10^{-3}$, $r_{min}^{(2)}(0.10) \sim 1.3\times10^{-3}$, and $r_{min}^{(1)}(0.15) \sim 8.5\times10^{-3}$, $r_{min}^{(2)}(0.15) \sim 3\times10^{-3}$. The cutoffs for $x>0.05$ are different because of apparent strong rounding.

and its frequency temperature dependence $f_G(T)$ (Fig. 3) is relatively, weakly affected by x. Also the transition temperature is relatively, weakly shifted ($\Delta T_{AC} < 0.2$ K, see Fig. 3). This indicates that the sample response is dominated by domains with bulklike ordering. The domains must be large enough in comparison to the pitch size so that long wave length Goldstone modes still exist. The reduction of the Goldstone and soft mode strength with increasing x originates partially in the formation of smaller domains where fluctuation pinning is effective and in increasing departures of preferred domain orientations from the z axis. Photopyroelectric measurements [4] reveal that with increased x the distribution of domain orientations strongly broadens (i.e., at $\rho_s \sim 0.04$ almost isotropic distribution is already reached). Consequently the effective polarization along the y direction is progressively reduced with increased x and due to this also the measured dielectric response.

In the regime $x < 0.15$ the strength of both modes is comparably suppressed with increased x. However the soft mode frequency f_s is dramatically affected by finite value of x close to the phase transition temperature (Fig. 3). For $x > 0$ the degeneracy between the soft and Goldstone mode frequencies at $T_{AC}(x)$ is lifted and the frequency gap between the modes increases with x. We believe that the reason behind this lies in the temperature dependent part of the τ_s dispersion relation [see Eq. (5)]. We claim that in different domains the effective temperature is slightly different. This might be due to the variation of the layer distance from a domain to a domain. The effect cannot be inferred from the free energy density expression described in Eq. (3) which assumes the equilibrium layer spacing. In order to understand consequences that layer compression or dilation can cause one must use the Landau-Ginzburg description of smectic ordering [26,27]. The smectic layering is modeled with a complex order parameter $\psi = \eta e^{i\varphi}$. Here the translational order parameter η describes the degree of smectic layering (for $\eta = 0$ the translational ordering is lost) and the phase factor φ determines the position of smectic layers: e.g., for layers stacked along the z direction at a distance $d_A = 2\pi/q_A$ it holds $\varphi = q_A z$. In this description the relevant free energy density term Δf that determines the equilibrium layer spacing and the tilt of molecules with respect to the layer normal can be expressed as

$$\Delta f = C_\| |(\vec{n} \cdot \nabla - iq_A)\psi|^2 + C_\perp |(\vec{n} \times \nabla)\psi|^2 + D|(\vec{n} \times \nabla)^2 \psi|^2.$$

$$(10)$$

The first two terms suffice to describe the ordering in the SmA phase in which the smectic compressibility ($C_\|$) and bend ($C_\perp$) elastic constants are positive. The first (compressibility) term drives the system towards the equilibrium SmA layer spacing q_A. The second (bend) terms enforces molecular orientation along the layer normal. This terms can drive the system into the smectic C phase if it becomes negative. Therefore setting $C_\perp = C_\perp^{(0)}(T - T_{AC})$ the second-order SmA-SmC (or SmA-SmC*) phase transition is realized at $T = T_{AC}$. Below T_{AC} the third term in Eq. (10) with elastic constant D is needed to stabilize the tilt θ below $\pi/2$.

For $\varphi = q_A z$, small values of θ, and neglecting spatial variations in ψ, one finds $\Delta f \sim \alpha(T - T_{AC})\theta^2 + \beta\theta^4$, where $\alpha = \eta^2 q_A^2 C_\perp^{(0)}$ and $\beta = D\eta^2 q_A^4$. This form of free energy yields for undistorted layers in the SmA phase the second order AC phase transition at $T = T_{AC}$: $\theta(T \geq T_{AC}) = 0$ and $\theta(T \leq T_{AC}) = \sqrt{\alpha(T_{AC} - T)/(2\beta)}$. For distorted layers, where $\varphi = qz$ and $q \neq q_A$, additional terms appear in Δf. Up to the second order in θ we get $\Delta f \sim \alpha(T - T_{AC})\theta^2 + C_\|\eta^2 q_A(q_A - q)\theta^2 = \alpha[T - (T_{AC} - \Delta T_{AC})]\theta^2$. The quantity

$$\Delta T_{AC} = \frac{C_\|}{C_\perp^{(0)}} \frac{q(q - q_A)}{q_A^2} \sim T_{AC}(q/q_A - 1) \qquad (11)$$

describes the temperature shift of the SmA-SmC* phase transition due to the homogeneous layer distortion. In Eq. (11) we assumed comparable smectic compressibility and bend elastic constants deep in the SmA phase (i.e., $C_\| \sim C_\perp^{(0)} T_{AC}$ and $q \sim q_A$). Note that even for a relatively small layer mismatch $q/q_A \sim 1.001$ one finds a detectable temperature shift: $\Delta T_{AC} \sim T_{AC}(q/q_A - 1) > 0.1$ K, $T_{AC} \sim 300$ K. This range of temperature shifts is comparable with our data (see Fig. 3) for $x > 0.025$. Note that for typical values of material constants [28] in Eq. (5) $[a_0 \sim 5 \times 10^{-5}$ J/(m^{2}K), $\nu \sim 0.1$ Ns/m$^2]$ one finds for $\Delta T \sim 0.1$ K the frequency shift $\Delta f_s \sim a_0 \Delta T/2\pi\gamma \sim 10$ kHz. This value roughly matches the observed frequency gaps between the soft and Goldstone modes at $T = T_{AC}^{(0)}$ for $x > 0$. Therefore the observed finite gap at the phase transition region can be attributed to a distribution of domain bulklike phase transitions.

The temperature dependence of the statical susceptibility $\varepsilon'(\omega = 0)$ can reveal the universality class to which our system belongs. Our analysis indicates that the critical exponent γ strongly depends on the temperature interval $(T_{\min}, T_{\max})$ in which the scaling exponent was extracted from measurements. For two different temperature intervals, determined by $r_{\min}^{(1)}(x) = (T_{AC} - T_{\min}^{(1)})/T_{\min}^{(1)}$ and $r_{\min}^{(2)}(x) = (T_{AC} - T_{\min}^{(2)})/T_{\min}^{(2)}$, both of which are sensible, we get completely different trends of $\gamma(x)$ dependence as x in increased. Here $r_{\min}^{(1)}(x = 0 - 0.05) \sim 2 \times 10^{-3}$, $r_{\min}^{(2)}(x = 0 - 0.05) \sim 5 \times 10^{-4}$, $r_{\min}^{(1)}(0.10) \sim 2.7 \times 10^{-3}$, $r_{\min}^{(2)}(0.10) \sim 1.3 \times 10^{-3}$, and $r_{\min}^{(1)}(0.15) \sim 8.5 \times 10^{-3}$, $r_{\min}^{(2)}(0.15) \sim 3 \times 10^{-3}$. For $x = 0$ both cases yield known pure-bulk value of $\gamma \sim 1$, consistent with the mean-field prediction. For $r_{\min}^{(1)}$ the $\gamma(x)$ dependence increases with x tentatively approaching the 3DXY universality class (in which $\gamma \sim 1.316$) as suggested also by other studies [2,7] that were focused to the N-SmA phase transition. The approaching towards 3DXY behavior with increasing x appears because the "impurities" are believed to effectively decuple the fluctuations in the smectic and nematic order parameter. Namely in the pure system with narrow nematic phase the coupling of these fluctuations is believed to cause departure from the 3DXY universality class. In fact our measurement can not exclude approaching to the random field Ising universality class with $\gamma = 1.8$. However for $r_{\min}^{(2)}$ completely different trend of $\gamma(x)$ dependence is observed within 95% confidence level. With decreased value of $r_{\min}$ the value

of $\gamma(x)$ decreases due to the smearing rounding effect in the $\varepsilon'(T)$ dependence close to the phase transition. For $r_{\min}^{(1)}$ the value of γ is already stable against the temperature range shrinkage.

Note that layer distortions can also affect the measured critical behavior at T_{AC}. The behavior across the second order SmA-SmC* phase transition is sensitive to the width of the Ginzburg temperature regime ΔT_G in which deviations from the mean-field behavior are expected. The criterion [29] can be expressed as $\Delta T_G = [k^2 T_C/(16\pi)^2](1/\Delta C_V^2 \xi_0^6)$, where ξ_0 is the bare smectic order parameter correlation length, ΔC_V the step in the specific heat at the critical temperature T_C as it is given by the mean-field theory, and k is the Boltzmann constant. Expression for ΔC_V and ξ_0 can be expressed with the Landau coefficients which get renormalized if layers are distorted. Consequently the Ginzburg criterion can be changed as demonstrated in Ref. [12].

VI. CONCLUSIONS

We have studied the influence of aerosil particles concentrations on the soft mode and Goldstone mode dynamics across the SmA-SmC* phase transition of the CE8 liquid crystal. The aerosil inclusions are spherical in shape with a characteristic radius R~7 nm. Their surface enforces strong homeotropic orientational anchoring. We studied concentrations $x = 0.025, 0.05, 0.1$, and 0.15. The complex dielectric constant was measured with dielectric spectroscopy. The mixtures were confined to plane parallel cells with smectic layers running perpendicular to the cell plates. The measuring low-frequency field was applied along the cell plates normal. Consequently the soft and Goldstone mode dynamics was probed at the wave vector $q \sim 0$.

Our measurements reveal that for $x < 0.15$ the Goldstone characteristic frequency f_G exhibits the bulklike behavior. Contrary at $T = T_{AC}$ the characteristic soft mode frequency f_s exhibits a gap $\Delta f_s(x)$ with respect to f_G. The gap gradually increases with x from $\Delta f_s(x=0)=0$ to $\Delta f_s(x=0.15)$ ~ 50 kHz. The strength of both modes monotonically decreases with x. For $x = 0.15$ the Goldstone mode disappears and the soft mode anomalously broadens. The results can be explained by assuming that the main contributions come from bulklike domains in the sample in which pining of fluctuations by impurities (i.e., aerosils) is negligible. Note that the established domain structure is rather strongly locked in by the silica network for $x > 0.10$. This can be inferred from approximately the same dielectric response from the "virgin" samples and the samples, that were exposed to the strong orienting magnetic field of 9 T prior to measurements.

The strength of modes decreases because the number of these domains, which only contribute to our measurements, is gradually decreasing. In addition the distribution of rela-tive orientation of domains is gradually approaching random distribution with x that also decreases modes' strengths. The gap $\Delta f(x) > 0$ for $x > 0$ arises due to the local spread of the transition temperatures caused by a slightly different smectic layer spacing in different domains. This behavior is for $x < 0.15$ enabled by "soft" character of the aerosil network enabling it to rearrange into spatially inhomogeneous distribution to reduce the imposed elastic strain. At $x = 0.15$ the aerosil network becomes "stiff," introducing more or less quenched disorder to surrounding LC phase. Consequently the temperature dependence of the soft mode strength anomalously broadens across the phase transition and the Goldstone mode is completely suppressed. It is to be stressed that in several cases we checked the dielectric response of samples also after being in a strong 9 T orienting magnetic field. The dielectric response of "oriented" and "virgin" samples was the same within the experimental error for $x \geq 0.10$, thus demonstrating the dominance of the stiff quenched disorder over the soft annealing character of the aerosil network. Note that in the stiff regime the broadening is also influenced by the presence of the LC phase whose behavior is strongly affected by the silica network. This is suggested also from the deviations from the Arrhenius behavior in the soft mode frequency temperature behavior observed with increasing x. The value of the soft mode frequency actually increases at higher temperatures, while at low temperatures due to the bending deviations from Arrhenius behavior (typically for glassy systems) the soft mode frequency becomes smaller than for pure bulk sample.

Relatively sharp $\varepsilon'(T)$ dependence across the SmA-SmC* phase transition enables us to extract the critical exponent γ revealing the universality class of our system. Our analysis indicates that the measured value of $\gamma(x)$ for $x > 0$ strongly depends on the temperature range used in the fitting. For measurements relatively far from T_{AC} ($r_{\min}^{(1)} \geq 2 \times 10^{-3}$), $\gamma(x)$ monotonically increases with x. For $x > 0.025$ values of γ seem to be consistent with the 3DXY model, as suggested also by other authors from studies on similar systems [7,2]. However for measurements closer to T_{AC} substantially lower values of γ are obtained. For $r_{\min}^{(2)} \geq 5 \times 10^{-4}$ the $\gamma(x)$ dependence even monotonically decreases with increasing x. Therefore our results indicate that measurements of critical exponents have to be taken with particular care. Note that similar behavior is found in relaxor materials [30].

[1] *Liquid Crystals in Complex Geometries Formed by Polymer and Porous Networks*, edited by G.P. Crawford and S. Žumer (Taylor and Francis, London, 1996).

[2] G.S. Iannacchione, C.W. Garland, J.T. Mang, and T.P. Rieker, Phys. Rev. E **58**, 5966 (1998), and references therein.

[3] P.G. de Gennes and J. Prost, *The Physics of Liquid Crystals* (Oxford University Press, Oxford, 1993).

[4] M. Marinelli, A.K. Ghosh, and F. Mercuri, Phys. Rev. E **63**, 061713 (2001).

[5] A. Hourri, T.K. Bose, and J. Thoen, Phys. Rev. E **63**, 051702 (2001).

[6] B. Zhou, G.S. Iannacchione, C.W. Garland, and T. Bellini, Phys. Rev. E **55**, 2962 (1997).

[7] H. Haga and C.W. Garland, Phys. Rev. E **56**, 3044 (1997).

[8] S.L. Messieh, J. Werner, H. Schmalfuss, W. Weissflog, and H. Kresse, Liq. Cryst. **26**, 535 (1999).

[9] M. Marinelli, A.K. Ghosh, and F. Mercuri, Phys. Rev. E **63**, 061713 (2001).

[10] C.C. Retsch, I. McNulty, and G.S. Iannacchione, Phys. Rev. E **65**, 032701 (2002).

[11] D.J. Cleaver, S. Kralj, T.J. Sluckin, and M.P. Allen, in *Liquid Crystals in Complex Geometries Formed by Polymer and Porous Networks*, edited by G.P. Crawford and S. Žumer (Taylor and Francis, London, 1996), p. 467.

[12] L. Benguigui and P. Martinoty, Phys. Rev. Lett. **63**, 774 (1989), and references therein.

[13] R. Blinc, M. Čopič, I. Drevenšek, A. Levstik, I. Muševič, and B. Žekš, Ferroelectrics **133**, 59 (1991).

[14] N.A. Clark and T.P. Rieker, Phys. Rev. A **37**, 1053 (1988).

[15] W.L. McMillan, Phys. Rev. A **8**, 1921 (1973).

[16] B.I. Halperin, T.C. Lubensky, and S.K. Ma, Phys. Rev. Lett. **32**, 292 (1974).

[17] R. Blinc and B. Žekš, Phys. Rev. A **18**, 740 (1978).

[18] B. Žekš, Mol. Cryst. Liq. Cryst. **114**, 259 (1984).

[19] Degussa Corp., Silica Division, 65 Challenger Rd., Ridgefield Park, NJ 07660.

[20] A. Levstik, Z. Kutnjak, C. Filipič, I. Levstik, Z. Bregar, B. Žekš, and T. Carlsson, Phys. Rev. A **42**, 2204 (1990).

[21] C.C. Huang and J.M. Viner, Phys. Rev. A **25**, 3385 (1982).

[22] T. Carlsson, B. Žekš, C. Filipič, and A. Levstik, Phys. Rev. A **42**, 877 (1990), and references therein.

[23] Z. Kutnjak, A. Levstik, and B. Žekš, Liq. Cryst. **8**, 589 (1990).

[24] As far as the Goldstone mode frequency is concerned, no particular changes were observed up to $x = 0.10$. The magnitude of the Goldstone mode frequency further away from T_{AC} remains to be in range $2-3$ kHz. For $x = 0.10$ it slightly exceeds 3 kHz. However, it should be noted that at $x = 0.10$ the intensity of the Goldstone mode becomes very small in comparison to the soft mode. This makes the separation of two modes more difficult. The observed increase in the Goldstone mode frequency for $x = 0.10$ could easily be an artificial effect. Namely, the much larger high frequency soft mode could slightly bias the value of the Goldstone mode frequency during the two modes separation process.

[25] C. Bagnuls and C. Bervillier, Phys. Rev. B **32**, 7209 (1985).

[26] S.R. Renn and T.C. Lubensky, Phys. Rev. A **38**, 2132 (1988).

[27] S. Kralj and T.J. Sluckin, Phys. Rev. E **50**, 2940 (1994).

[28] T. Carlsson and I. Dahl, Mol. Cryst. Liq. Cryst. **95**, 373 (1983).

[29] V.L. Ginzburg, Fiz. Tverd. Tela **2**, 2031 (1960) [Sov. Phys. Solid State **2**, 1824 (1960)].

[30] D. Viehland, S.J. Jang, L.E. Cross, and M. Wuttig, Phys. Rev. B **46**, 8003 (1992).